Supplementary Materials for

Purcell-enhanced Ultrasound Emission by Perfluorocarbon Nanodroplets

Tianye Zhang[1], John Kim[1, †], Heidi Zhang[1], Ge Wang[1], Ke Ding[1], Yan Deng[1], Chenzhe Wang[1], Jianyu Hua[1], Chengzhi Shi[1*]

[†]These authors contributed equally to this work.

[1]Department of Mechanical Engineering, University of Michigan, Ann Arbor, MI, 48109, USA

[*]Corresponding author: czshi@umich.edu

This PDF file includes:

Supplementary Materials 1

Derivation for acoustic Purcell effect for point source

Starting with the first-order wave equation for a point source

$$\nabla^2 p - \frac{1}{c_{\text{air}}^2}\frac{\partial^2 p}{\partial t^2} = -\rho_{\text{air}}\frac{\partial Q(t)}{\partial t}\delta(\vec{r} - \vec{r_0}) \tag{1}$$

The Green's function $G(\omega, r, r_0)$ satisfies:

$$\nabla^2 G(\omega, r, r_0) + k^2 G(\omega, r, r_0) = \delta(r - r_0) \tag{2}$$

Where $k^2 = \omega^2/c_0^2$. Using this Green's function, the pressure at the source location can be given as the following:

$$p_s = i\omega\rho_0 u_s S_s G(\omega, r = r_0, r_0) \tag{3}$$

To compute the emission power, we integrate the time-averaged energy flux over the source surface:

$$P = 0.5\omega\rho_0 u_s S_s u_s^* S_s \text{Re}\{iG(\omega, r = r_0, r_0)\}. \tag{3}$$

From the definition of density of states (DOS)

$$\xi = -\frac{dk_0^2(\omega)}{d\omega}\frac{1}{\pi}\text{Im}\{G(\omega, r = r_0, r_0)\} \tag{4}$$

The final power expression can be found after simplification to be:

$$P = \frac{\pi\rho_0 c_0^2 |Q|^2 \xi(\omega)}{4} \tag{5}$$

And thus the final acoustic Purcell factor (APF) is defined as:

$$\text{APF} = \left(\frac{P_{\text{structure}}}{P_0}\right)^2 \tag{6}$$

Supplementary Materials 2

Derivation of Wave Equation for Microbubble Medium

Consider the three-dimensional case of acoustic wave propagation. Microbubbles inside hydrogels can be simplified as a mixture of water and gas. When the number of bubbles per unit volume is relatively small, the hydrodynamic properties of the mixture differ only slightly from those of pure water. The governing equations and the second-order approximate dynamic equations are given as follows.

$$\frac{\partial u}{\partial t} + u \cdot \nabla u = -\frac{1}{\rho_0}\nabla p + \frac{1}{\rho_0}\left(\frac{4}{3}\eta' + \eta'' + \frac{\gamma - 1}{P_r}\right)\nabla^2 u \tag{7}$$

$$\frac{\partial \rho}{\partial t} + \nabla \cdot (\rho_0 u) = 0 \tag{8}$$

$$p = c_0^2 \rho' + \frac{(B/A)_L}{2\rho_0} c_0^2 \rho'^2 \tag{9}$$

where $\rho' = \rho - \rho_0$ is the density perturbation. The effective density of the bubbly mixture is defined as:

$$\rho_e = \rho_g Z + \rho_0 (1 - Z) \tag{10}$$

where Z is the gas volume fraction, given by:

$$Z = n(V' + V_0) \tag{11}$$

Differentiating with respect to time:

$$\frac{\partial \rho_e}{\partial t} = (\rho_g - \rho_0) n \frac{\partial V'}{\partial t} \tag{12}$$

Taking the second time derivative:

$$\frac{\partial^2 \rho_e}{\partial t^2} = (\rho_g - \rho_0) n \frac{\partial^2 V'}{\partial t^2} \tag{13}$$

From the continuity equation:

$$\frac{\partial \rho}{\partial t} + \nabla \cdot (\rho_0 u) = 0 \tag{14}$$

Expanding ($\rho = \rho_e + \rho'$), we obtain:

$$\frac{\partial \rho_e}{\partial t} + \frac{\partial \rho'}{\partial t} + \nabla \cdot (\rho_0 u) = 0 \tag{15}$$

Taking the second time derivative:

$$\frac{\partial^2 \rho_e}{\partial t^2} + \frac{\partial^2 \rho'}{\partial t^2} + \nabla \cdot \frac{\partial (\rho_0 u)}{\partial t} = 0 \tag{16}$$

Substituting the effective density relation:

$$(\rho_g - \rho_0) n \frac{\partial^2 V'}{\partial t^2} + \frac{\partial^2 \rho'}{\partial t^2} + \nabla \cdot \frac{\partial (\rho_0 u)}{\partial t} = 0 \tag{17}$$

And we can obtain the relation between pressure and density

$$\frac{\partial^2 \rho'}{\partial t^2} = -(\rho_g - \rho_0) n \frac{\partial^2 V'}{\partial t^2} - \nabla \cdot \frac{\partial (\rho_0 u)}{\partial t} = 0 \tag{18}$$

Taking the time derivative of the equation of state:

$$\frac{\partial p}{\partial t} = c_0^2 \frac{\partial \rho'}{\partial t} + \frac{(B/A)_L}{\rho_0} c_0^2 \rho' \frac{\partial \rho'}{\partial t} \tag{19}$$

Taking the second time derivative:

$$\frac{\partial^2 p}{\partial t^2} = c_0^2 \frac{\partial^2 \rho'}{\partial t^2} + \frac{(B/A)_L}{\rho_0} c_0^2 \left(\rho' \frac{\partial^2 \rho'}{\partial t^2} + \left(\frac{\partial \rho'}{\partial t} \right)^2 \right) \tag{20}$$

Solving for $\frac{\partial^2 \rho'}{\partial t^2}$:

$$\frac{\partial^2 \rho'}{\partial t^2} = \frac{1}{c_0^2} \frac{\partial^2 p}{\partial t^2} - \frac{(B/A)_L}{\rho_0 c_0^2} \left(\rho' \frac{\partial^2 \rho'}{\partial t^2} + \left(\frac{\partial \rho'}{\partial t} \right)^2 \right) \tag{21}$$

Substituting into the time-differentiated continuity equation:

$$(\rho_g - \rho_0) n \frac{\partial^2 V'}{\partial t^2} + \frac{1}{c_0^2} \frac{\partial^2 p}{\partial t^2} - \frac{(B/A)_L}{\rho_0 c_0^4} \left(\rho' \frac{\partial^2 p}{\partial t^2} + \left(\frac{\partial p}{\partial t} \right)^2 \right) + \nabla \cdot \frac{\partial (\rho_0 u)}{\partial t} = 0 \tag{22}$$

Using the divergence of the momentum equation:

$$\nabla \cdot \frac{\partial u}{\partial t} = -\frac{1}{\rho_0} \nabla^2 p + \frac{b_0}{\rho_0} \nabla^2 \frac{\partial p}{\partial t} \tag{23}$$

Where $b_0 = \frac{1}{\rho_0} \left(\frac{4}{3} \eta' + \eta'' + \frac{\gamma - 1}{P_r} \right)$. Substituting, we have found the nonlinear second order wave equation for bubbly fluids:

$$\nabla^2 p - \frac{1}{c_0^2} \frac{\partial^2 p}{\partial t^2} = -\rho_0 n \frac{\partial^2 V'}{\partial t^2} - \frac{(B/A)_L}{\rho_0 c_0^4} \left(\rho' \frac{\partial^2 p}{\partial t^2} + \left(\frac{\partial p}{\partial t} \right)^2 \right) - b_0 \nabla^2 \frac{\partial p}{\partial t} \tag{24}$$

Considering the emitted pressure of bubbles, the amplitude of the main harmonic can be assumed to be larger than other harmonics. Thus, we can linearize and look at the first-order wave equation for bubbly fluids, as shown below:

$$\nabla^2 p - \frac{1}{c_0^2}\frac{\partial^2 p}{\partial t^2} = -\rho_0 n \frac{\partial^2 V'}{\partial t^2} - -b_0 \nabla^2 \frac{\partial p}{\partial t} \tag{25}$$

The Rayleigh-Plesset equation describes the radial motion of a gas bubble in a liquid:

$$R\ddot{R} + \frac{3}{2}\dot{R}^2 = \frac{1}{\rho_D}\left(P_i - P(t) - \frac{2\sigma}{R} - \frac{4\eta'}{R}\dot{R}\right) \tag{26}$$

where R is the bubble radius, ρ_d is the density of the surrounding liquid, P_i is the internal bubble pressure, $P(t)$ is the external bubble pressure, σ is the surface tension, η' is the liquid viscosity.

The volume of the spherical bubble is given by:

$$V = \frac{4}{3}\pi R^3 \tag{27}$$

We define the volumetric perturbation as:

$$V' = V - V_0 \tag{28}$$

where $V_0 = \frac{4}{3}\pi R_0^3$ is the equilibrium volume. For small radial perturbations, we approximate:

$$R = R_0 + R' \tag{29}$$

And expand:

$$V' = \frac{4}{3}\pi(R_0 + R')^3 - \frac{4}{3}\pi R_0^3 \tag{30}$$

Using a Taylor series expansion:

$$(R_0 + R')^3 = R_0^3 + 3R_0^2 R' + 3R_0 R'^2 + R'^3 \tag{31}$$

and neglecting the second and higher-order terms, we can then obtain:

$$V' \approx 4\pi R_0^2 R'. \tag{32}$$

Taking the second order derivative:

$$\ddot{V}' \approx 4\pi R_0^2 \ddot{R}' \tag{33}$$

We can obtain $\ddot{R}' = \frac{\ddot{V}'}{4\pi R_0^2}$ and substitute back into the Rayleigh-Plesset Equation. Assuming $V'/V \ll 1$ and preserving only second-order terms, we can rewrite it as:

$$\ddot{V}' + \omega_0^2 V' - \delta V'^2 - \beta\left(2V'\dot{V}' + (V')^2\right) + g\dot{V}' = -\epsilon p \tag{34}$$

Where $\omega_0^2 = \frac{3\gamma P_0}{\rho_0 R_0^2}, \quad \delta = 3\beta(\gamma+1)\omega_0^2, \quad \beta = \frac{1}{8\pi R_0^3}, \quad g = \frac{\omega}{Q}, \quad \epsilon = \frac{4\pi R_0}{\rho_0}$ and R_0 is the equilibrium radius and Q is the quality factor determined experimentally. Using a perturbation series expansion, we express the volumetric perturbation as:

$$V' = V_1' + V_2' + \cdots \tag{35}$$

And the pressure field as

$$p = p_1 + p_2 + \cdots \tag{36}$$

Preserving only the first and second order terms, the equations becomes:

$$\dot{V'}_1 + \omega_0^2 V_1' + g\dot{V'}_1 = -\epsilon p_1, \tag{37}$$

$$\dot{V'}_2\left(1 - \frac{1}{4z^2} - j\frac{1}{2Q}\right) - (\delta - 3\beta\omega^2)(V_1')^2 = -\epsilon p_2 \tag{38}$$

Where $z = \omega/\omega_0$. Solving for the first and second-order volumetric perturbations:

$$\dot{V'}_1 = \frac{-\epsilon p_1}{\left(1 - \frac{1}{z^2} + \frac{1}{j\omega}g\right)} \tag{39}$$

$$\dot{V'}_2 = \frac{-\epsilon p_2}{\left(1 - \frac{1}{4z^2} - j\frac{1}{2Q}\right)} + \frac{(\delta - 3\beta\omega^2)(V_1')^2}{\left(1 - \frac{1}{4z^2} - j\frac{1}{2Q}\right)} \tag{40}$$

The above two equations provide the first- and second-order volumetric oscillations and nonlinear effects in bubbly liquids. Substituting back into the first-order wave equation for bubbly liquids:

$$\frac{\partial^2 p_1}{\partial x^2} - \frac{1}{c_0^2}\frac{\partial^2 p_1}{\partial t^2} = \frac{\rho_0 n\varepsilon p_1}{\left(1 - \frac{1}{z^2} + j\frac{g}{\omega}\right)} - b_0\frac{\partial^3 p_1}{\partial t\,\partial x^2} \tag{41}$$

Where $z = \omega/\omega_0$.

To solve this wave equation, we assume a plane wave solution of the form:

$$p_1 = P_1 e^{j(\omega t - \widetilde{k_1} r)} \tag{42}$$

Where the complex wavenumber is given by

$$\widetilde{k_1^2} = A_1 - jB_1 \tag{43}$$

After substituting, we can solve the coefficients and find that:

$$A_1 = \frac{1}{1+\omega^2 b_0}\left\{k_0^2 - \frac{\rho_0 n\epsilon\left[\left(1-\frac{1}{z^2}\right)+\frac{\omega b_0}{Q}\right]}{\left(1-\frac{1}{z^2}\right)^2+\frac{1}{Q^2}}\right\} \tag{44}$$

$$B_1 = \frac{1}{1+\omega^2 b_0}\left\{k_0^2\omega b_0 - \frac{\rho_0 n\epsilon\left[\left(1-\frac{1}{z^2}\right)\omega b_0-\frac{1}{Q}\right]}{\left(1-\frac{1}{z^2}\right)^2+\frac{1}{Q^2}}\right\} \tag{45}$$

where $k_0 = \frac{\omega}{c_0}$.

To emphasize the impact of bubble resonance, we can set z=1 and simplify $b_0 = 0$. Then, the attenuation coefficient and wavenumber simplify to:

$$\alpha_1 = \frac{1}{\sqrt{2}}\left\{\sqrt{k_0^4 + \frac{(\rho_0 n\epsilon)^2 - 2k_0^2\rho_0 n\epsilon\left(1-\frac{1}{z^2}\right)}{\left(1-\frac{1}{z^2}\right)^2+\frac{1}{Q^2}}} - \left(k_0^2 - \frac{\rho_0 n\epsilon\left(1-\frac{1}{z^2}\right)}{\left(1-\frac{1}{z^2}\right)^2+\frac{1}{Q^2}}\right)\right\}^{1/2} \tag{46}$$

$$k_1 = \frac{B_1}{2\alpha_1} \tag{47}$$

This equation shows that the attenuation due to bubble oscillations depends strongly on frequency and exhibits resonance characteristics.

Supplementary Materials 3

Derivation of APF for Microbubble Medium

To find the emitted power of a microbubble, we start with the volumetric expansion of a previously derived bubble.

$$\ddot{V}_1' = \frac{-\epsilon p_1}{\left(1 - \frac{1}{z^2} + \frac{1}{j\omega} g\right)} \tag{48}$$

We know that for acoustic radiation, we need to acoustic for radiation resistance $R_s = \rho_0 c_0 (kR)^2 S$. Thus, we can solve for $V_1' = \frac{-\epsilon p_1}{(j\omega)^2\left(1 - \frac{1}{z^2} + \frac{1}{j\omega} g + \frac{R_s}{j\omega m_s}\right)}$ where $m_s = 4\pi R^3 \rho$. We can then calculate the displacement perturbation of the bubble surface:

$$u = \frac{V_1'}{4\pi R^2} = \frac{-\epsilon p_1}{4\pi R^2 (j\omega)^2 \left(1 - \frac{1}{z^2} + \frac{1}{j\omega} g + \frac{R_s}{j\omega m_s}\right)} \tag{49}$$

The velocity perturbation can then be found:

$$v_m = (j\omega) u = \frac{-j\omega \epsilon p_1}{4\pi R^2 (j\omega)^2 \left(1 - \frac{1}{z^2} + \frac{1}{j\omega} g + \frac{R_s}{j\omega m_s}\right)} \tag{50}$$

Simplifying,

$$v_m = \frac{-\epsilon p_1}{4\pi R^2 j\omega \left(1 - \frac{1}{z^2} + \frac{1}{j\omega} g + \frac{R_s}{j\omega m_s}\right)} \tag{51}$$

Where $p_1 = P_1 e^{-j\widetilde{k_1} r}$.

The radiated acoustic power from a single bubbles is given as

$$P_s = \frac{1}{2} v_m^2 R_s \tag{52}$$

Where $R_s = \rho_0 c_0 S (kR)^2, \epsilon = \frac{4\pi R}{\rho_0}, g = \frac{\omega_0}{Q}$.

Subtituting v_m,

$$P_s = \frac{2\pi P_1^2 e^{-2j\widetilde{k_1} r} c_0 (kR)^2}{\rho_0 \omega^2 \left|1 - \frac{1}{z^2} + \frac{1}{j\omega} g + \frac{R_s}{j\omega m_s}\right|^2}. \tag{53}$$

The incident power intensity is:

$$P_0 = \frac{1}{2}\frac{P_1^2 S}{\rho_0 c_0} \tag{54}$$

Thus, the Acoustic Purcell Factor (APF) for a single microbubble medium is

$$\mathrm{APF} = \xi = e^{-2j\widetilde{k_1}r}\frac{1}{\left(1 - \frac{1}{z^2} + \frac{1}{j\omega}g + \frac{(k^2 R c_0)}{j\omega}\right)^2}. \tag{55}$$

Assuming we have n same radius bubbles that are uniformly dispersed, we can disregard the effects of multi-scattering and thus the APF for bubbly liquids with concentration n is:

$$\mathrm{APF} = \xi = e^{-2j\widetilde{k_1}r}\frac{n}{\left(1 - \frac{1}{z^2} + \frac{1}{j\omega}g + \frac{(k^2 R c_0)}{j\omega}\right)^2}. \tag{56}$$

Supplementary Materials 4

Derivation of Wave Equation for Nanodroplet Medium

The radial dynamics of a nanodroplet under acoustic excitation are given by

$$\rho_0\left(R\ddot{R}+\frac{3}{2}\dot{R}^2\right)=-\rho_1 k_1 c_1^2\frac{j_0(X)}{j_1(X_0)}(R-R_0)-4(\mu_0-\mu_1)\frac{\dot{R}}{R}-2\sigma\left(\frac{1}{R}-\frac{1}{R_0}\right)-p(t) \quad (57)$$

where ρ_1, c_1 are the internal density and sound speed, μ_0 and μ_1 are the external and internal viscosities, σ is surface tension, R_0 is the equilibrium radius, and $p(t)$ is the acoustic pressure. For small perturbations $R(t)=R_0+r(t)$, linearization gives

$$\rho_0 R_0\ddot{r}+\frac{4(\mu_0-\mu_1)}{R_0}\dot{r}+\left(\frac{2\sigma}{R_0^2}+\rho_1 k_1 c_1^2\frac{j_0(X_0)}{j_1(X_0)}\right)r=-p(t) \quad (58)$$

Expressing the volume perturbation $V'\approx 4\pi R_0^2 r$

$$\ddot{V}'+\gamma_d\dot{V}'+\omega_d^2 V'=-\epsilon p(t) \quad (59)$$

With parameters $\epsilon=\frac{4\pi R_0}{\rho_0}$, $\gamma_d=\frac{4(\mu_0-\mu_1)}{\rho_0 R_0^2}$, and $\omega_d^2=\frac{1}{\rho_0 R_0}\left(\frac{2\sigma}{R_0^2}+\rho_1 k_1 c_1^2\frac{j_0(X_0)}{j_1(X_0)}\right)$.

Introducing the normalized frequency $z = \omega/\omega_d$ and quality factor $Q_d=\omega_d/\gamma_d$, we obtain

$$\tilde{k}^2=\frac{k_0^2}{1+j\omega b_0}\left[1+\rho_0 n\epsilon\,\frac{\left(1-\frac{1}{z^2}\right)+j\frac{1}{Q_d z}}{\left(1-\frac{1}{z^2}\right)^2+\left(\frac{1}{Q_d z}\right)^2}\right]. \quad (60)$$

Separating into real and imaginary parts, $\tilde{k}^2=A_1-jB_1$ gives the phase velocity and attenuation of waves in a nanodroplet medium where

$$A_1=\frac{k_0^2}{1+x^2}\,[\,1+S_r+x\,S_i\,]=\frac{k_0^2}{1+\omega^2 b_0^2}\left\{1+\rho_0 n\epsilon\,\frac{1-\backslash dfrac1z^2}{D_d}+\omega b_0\,\rho_0 n\epsilon\,\frac{1}{Q_d z\,D_d}\right\} \quad (61)$$

$$B_1=\frac{k_0^2}{1+x^2}\,[\,x(1+S_r)-S_i\,]=\frac{k_0^2}{1+\omega^2 b_0^2}\left\{\omega b_0\left[1+\rho_0 nc\,\frac{1-\backslash dfrac1z^2}{D_d}\right]-\rho_0 nc\,\frac{1}{Q_d\,z\,D_d}\right\} \quad (62)$$

Supplementary Materials 5

Derivation of APF for Nanodroplet Medium

The dynamics of a nanodroplet under acoustic excitation can be described by the following equation:

$$\rho_0\left(R\ddot{R}+\frac{3}{2}\dot{R}^2\right)=-\rho_1 k_1 c_1^2\frac{j_0(X)}{j_1(X_0)}(R-R_0)-4(\mu_0-\mu_1)\frac{\dot{R}}{R}-2\sigma\left(\frac{1}{R}-\frac{1}{R_0}\right)-p_A(t) \quad (63)$$

Where ρ_0 and c_0 are the density and speed of sound in the surrounding medium (e.g. water), ρ_1 and c_1 are the density and speed of sound in the nanodroplet (e.g. perfluoropentane), μ_0 and μ_1 are the viscosities of the surrounding medium and nanodroplet, σ is the surface tension, $k_1 = \omega_1 c_1$ inside the nanodroplet, $X = k_1 R$ and $X_0 = k_1 R_0$ are the dimensionless parameters, and $j_0(X)$ and $j_1(X)$ are the spherical Bessel functions of the first kind.

Assuming small oscillations around the equilibrium radius R_0, we can write:

$$R(t) = R_0 + \tilde{R}e^{i\omega t} \quad (64)$$

Differentiating with respect to time:

$$\dot{R} = i\omega\tilde{R}e^{i\omega t}, \quad \ddot{R} = -\omega^2\tilde{R}e^{i\omega t} \quad (65)$$

Substituting into the governing equation and neglecting nonlinear terms, we obtain:

$$\tilde{R} = \frac{p_A}{\rho_0 R_0\omega^2 - \rho_1 k_1 c_1^2\frac{j_0(X)}{j_1(X_0)} + \frac{4i\omega(\mu_0-\mu_1)}{R_0} + \frac{2\sigma}{R_0^2}} \quad (66)$$

Thus, the velocity of the droplet surface is:

$$\dot{R} = i\omega\tilde{R}e^{i\omega t} \quad (67)$$

The emitted acoustic power is given by:

$$P_r = \frac{1}{2}\dot{R}^2 R_s \quad (68)$$

Where the radiation resistance is $R_s = \rho_0 c_0 S(kR)^2$.

Substituting $\dot{R}$, we obtain the expression for emitted acoustic power for the nanodroplet medium:

$$P_r = \frac{1}{2}\frac{\omega^2 p_A^2 \rho_0 c_0 S\left(\tilde{k}R\right)^2}{\left|\rho_0 R_0\omega^2 - \rho_1 k_1 c_1^2\frac{j_0(X)}{j_1(X_0)} + \frac{4i\omega(\mu_0-\mu_1)}{R_0} + \frac{2\sigma}{R_0^2}\right|^2} \quad (69)$$

Thus, the APF for nanodroplet medium while assuming n same radius nanodroplets that are uniformly dispersed and disregarding multi-scattering is:

$$\mathrm{APF} = \frac{n\omega^2 \rho_0 c_0 \left(\tilde{k}R\right)^2}{\rho_0 c_0 \left|\rho_0 R_0 \omega^2 - \rho_1 k_1 c_1^2 \frac{j_0(X)}{j_1(X_0)} + \frac{4i\omega(\mu_0 - \mu_1)}{R_0} + \frac{2\sigma}{R_0^2}\right|^2} \tag{70}$$

Supplementary Materials 6

Frequency dependence of APF for nanodroplet and microbubble medium

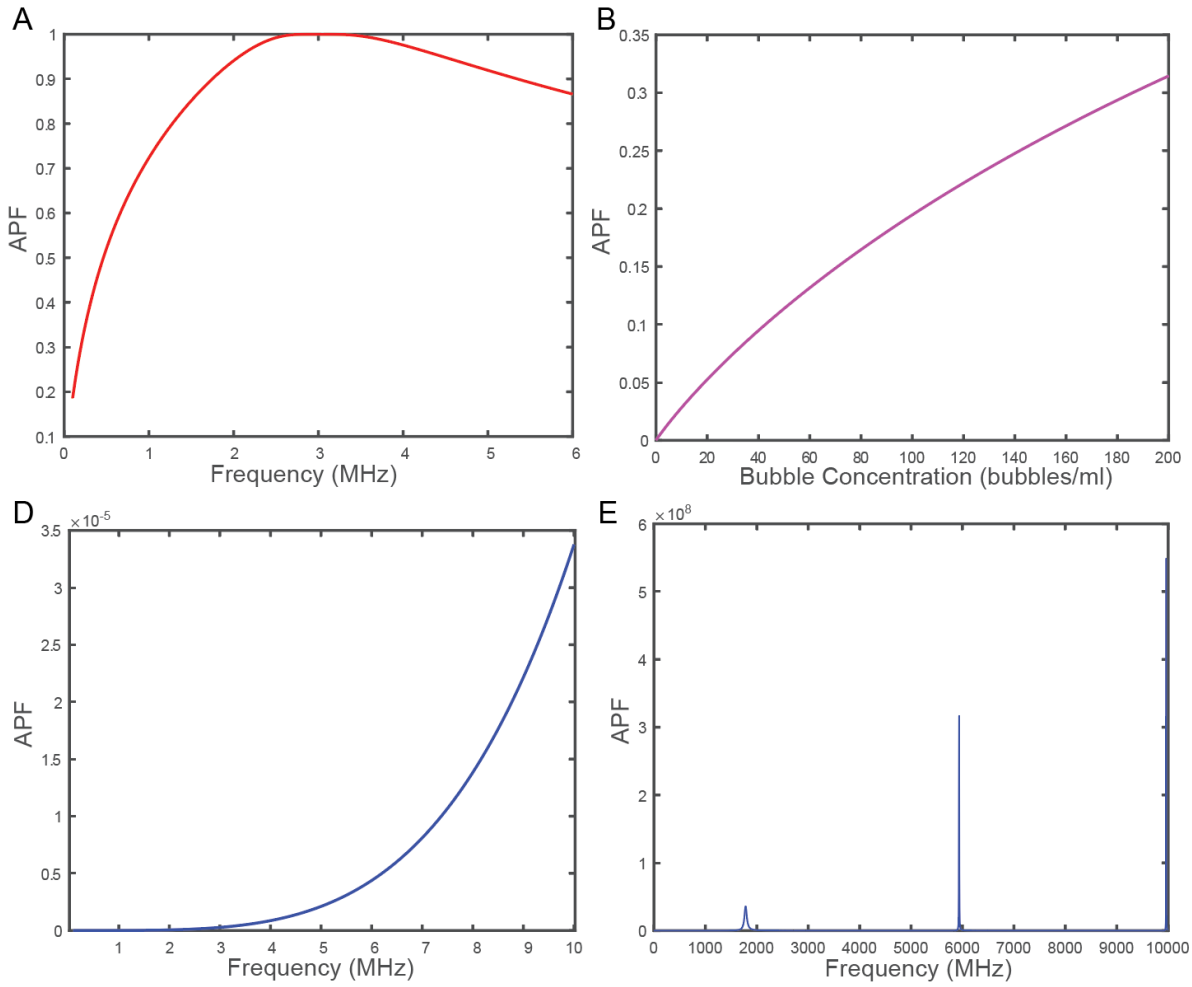

Fig S1: (A) Theoretical acoustic Purcell factor (APF) as a function of frequency (1–100 MHz) for a microbubble medium with fixed radius R=1 μm and concentration on n=10^8 **(B)** Theoretical APF as a function of microbubble concentration *n* ranging from 0 to 2×10^8 bubbles/m^3, evaluated at the resonance frequency of $\omega_0 = \sqrt{\frac{3\gamma P_0}{\rho_0 R^2}}$. **(C)** Frequency-dependent APF for a nanodroplet medium across microbubble resonance frequency range (1–10 MHz), with fixed radius R=100 nm. **(D)** Frequency-dependent APF for a nanodroplet medium across a broad frequency range (0–10 GHz), with fixed radius R=100 nm.

Supplementary Materials 7

Derivation of acoustic DOS for microbubble medium

The relationship of the emitted power P and the acoustic DOS ξ is given as follows:

$$P = \frac{\pi\rho_0 c_0^2 |Q|^2 \xi(\omega)}{4} \tag{71}$$

Sovling for ξ:

$$\xi(\omega) = \frac{4P}{\pi\rho_0 c_0^2 |Q|^2} \tag{72}$$

The radiated acoustic power for a single oscillating bubble is given as:

$$P = \left| \frac{2\pi P_1^2 e^{-2jk_r c_0 (kR)^2}}{\rho_0 \omega^2 \left(1 - \frac{1}{z^2} + \frac{1}{j\omega g} + \frac{R_s}{j\omega m_s}\right)} \right|^2 \tag{73}$$

Solving for ξ:

$$\xi(\omega) = \frac{4}{\pi\rho_0 c_0^2 |Q|^2} \cdot \left| \frac{2\pi P_1^2 e^{-2jk_r c_0 (kR)^2}}{\rho_0 \omega^2 \left(1 - \frac{1}{z^2} + \frac{1}{j\omega g} + \frac{R_s}{j\omega m_s}\right)} \right|^2 = \frac{4}{\pi\rho_0 c_0^2 |Q|^2} \cdot \left| \frac{4\pi^2 |P_1|^4 c_0^2 (kR)^2 e^{-4k_r'' r}}{\rho_0^2 \omega^4 \left|1 - \frac{1}{z^2} + \frac{1}{j\omega g} + \frac{R_s}{j\omega m_s}\right|^2} \right| \tag{74}$$

Finally, we have obtained the final relationship for the DOS of microbubble medium after simplification:

$$\xi(\omega) = \frac{16\pi |P_1|^4 (kR)^4}{\rho_0^3 \omega^4 |Q|^2} \left|1 - \frac{1}{z^2} + \frac{1}{j\omega g} + \frac{R_s}{j\omega m_s}\right|^{-2} \tag{75}$$

Supplementary Materials 8

The derivation of acoustic DOS for nanodroplet medium

The relationship between the emitted power of nanodroplet medium P and the acoustic DOS ξ is given as follows:

$$P_r = \frac{\pi\rho_0 c_0^2 |Q|^2 \xi(\omega)}{4} \tag{76}$$

Following the derivation above and considering the emitted power for nanodroplet medium:

$$P_r = \left| \frac{1}{2} \cdot \frac{\omega^2 T_A^2 \rho_0 c_0 S(kR)^2}{\rho_0 R_0 \omega^2 - \rho_1 h_1^2 k_1^2 c_1^2 \frac{j_0(X)}{j_1(X_0)} + \frac{4i\omega(\mu_0 - \mu_1)}{R_0} + \frac{2\sigma}{R_0^2}} \right|^2 \tag{77}$$

The final relationship for the DOS of nanodroplet medium can be found to be:

$$\xi(\omega) = \frac{\omega^4 T_A^4 \rho_0^2 c_0^2 S(kR)^4}{\pi\rho_0 c_0^2 |Q|^2 \left| \rho_0 R_0 \omega^2 - \rho_1 h_1^2 k_1^2 c_1^2 \frac{j_0(X)}{j_1(X_0)} + \frac{4i\omega(\mu_0 - \mu_1)}{R_0} + \frac{2\sigma}{R_0^2} \right|^2} \tag{78}$$

Supplementary Materials 9

Comparison of APF and scattering cross-sections for microbubbles

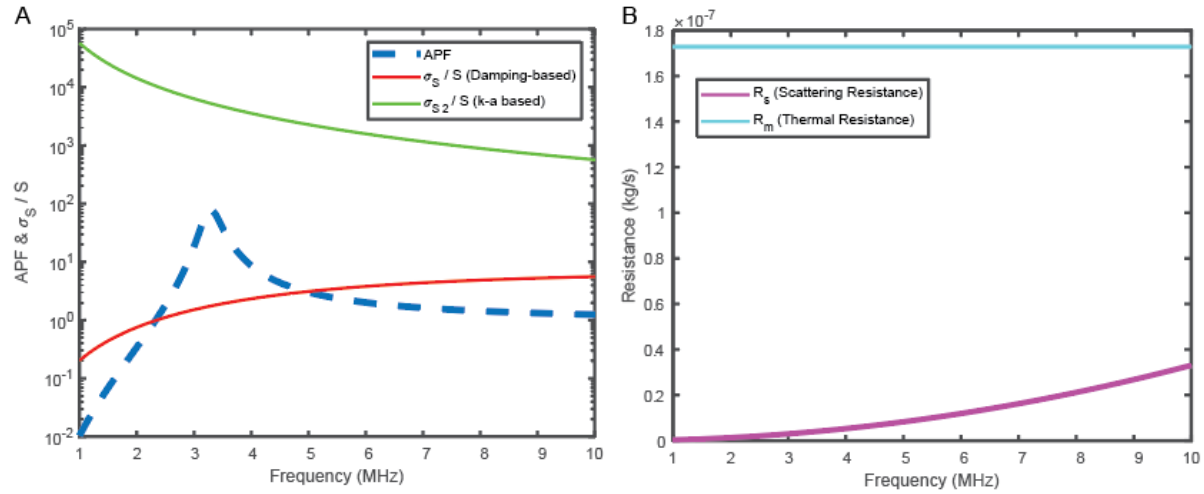

Fig S2: (A) Comparison of APF, scattering cross-section/S, and k-a based scattering cross-section/S **(B)** Comparison for scattering resistance, thermal resistance with respect to frequency.

Supplementary Materials 10

Spatial-domain filtering for B-mode imaging for agarose gel and agarose gel with nanodroplets

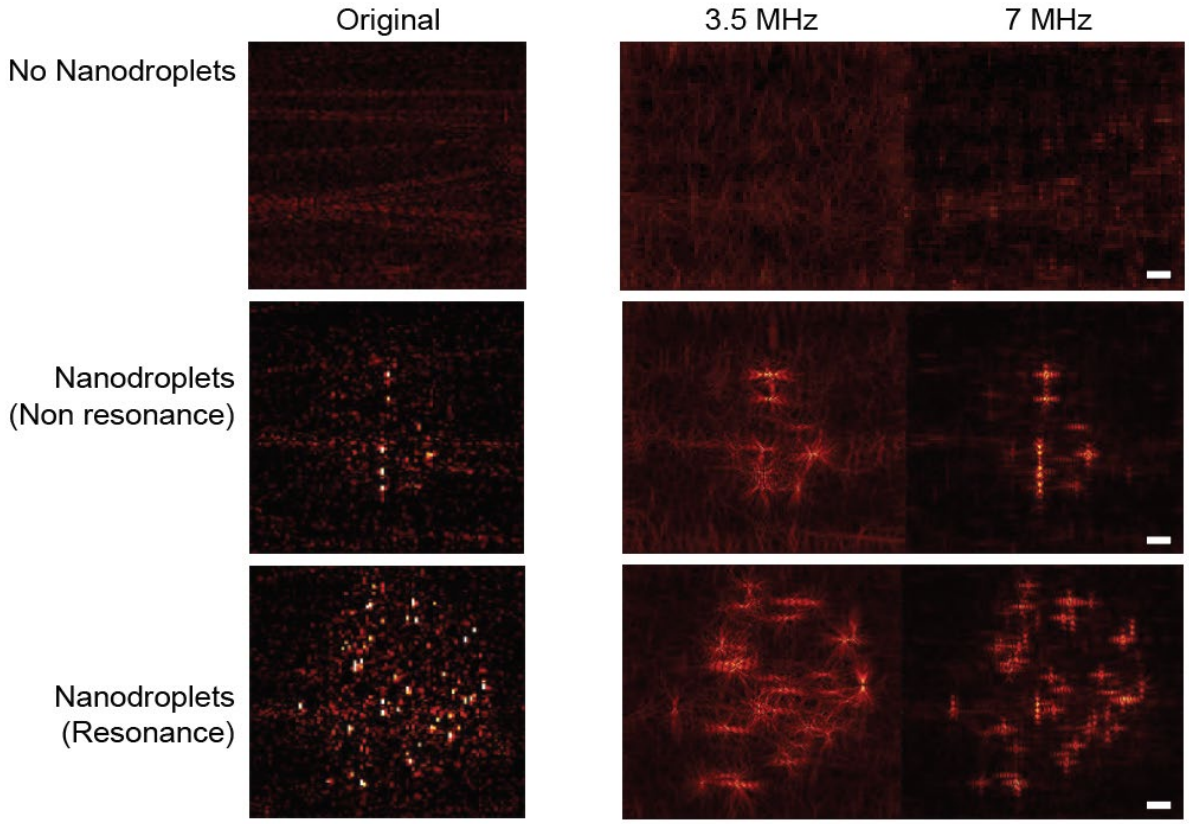

Fig S3: Spatial-domain filtered ultrasound images showing nanodroplet-mediated emission under different conditions. Representative images are shown for (top to bottom) no nanodroplets, nanodroplets (non-resonant condition), and nanodroplets (resonant condition) at original, 3.5 MHz, and 7 MHz frequencies. Spatial-domain filtering was applied for improved visualization of emission features. Stronger contrast and structured emission patterns are observed in the presence of nanodroplets, particularly under resonance. Other Additional imaging methods (e.g., frequency-domain filtering, adaptive beamforming, or super-resolution reconstruction) can also be applied to further enhance contrast, intensity, and resolution. Scale bars: 1 μm.

Supplementary Materials 11
Acoustic Purcell Factor (APF) during Acoustic Droplet Vaporization (ADV)

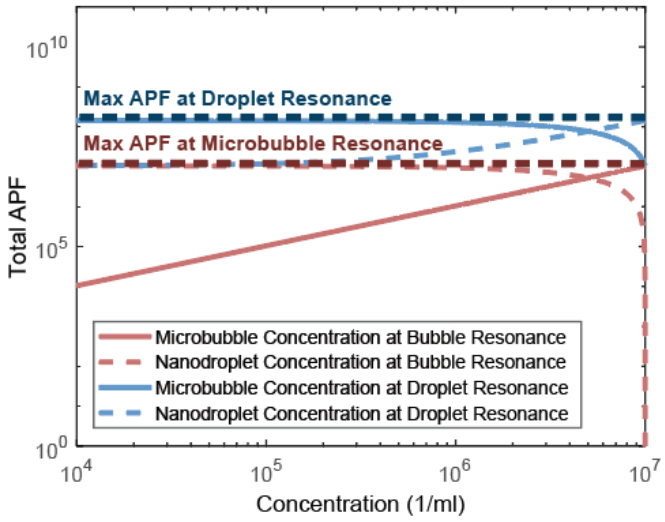

Fig S4: Simulation of APF evolution for nanodroplets and microbubbles under bubble resonance (red curves) and droplet resonance (blue curves). Solid lines represent microbubbles, while dashed lines represent nanodroplets. During ADV, nanodroplets undergo a transition from droplet to bubble resonance, leading to a sharp increase in APF and surpassing microbubble performance at higher driving pressures. This illustrates how the vaporization process fundamentally enhances emission efficiency, providing a physical basis for contrast enhancement in ultrasound imaging and therapy.

Supplementary Materials 12

Structural mechanism and performance landscape of Purcell-enhanced acoustic emission for lower concentration nanodroplet sample

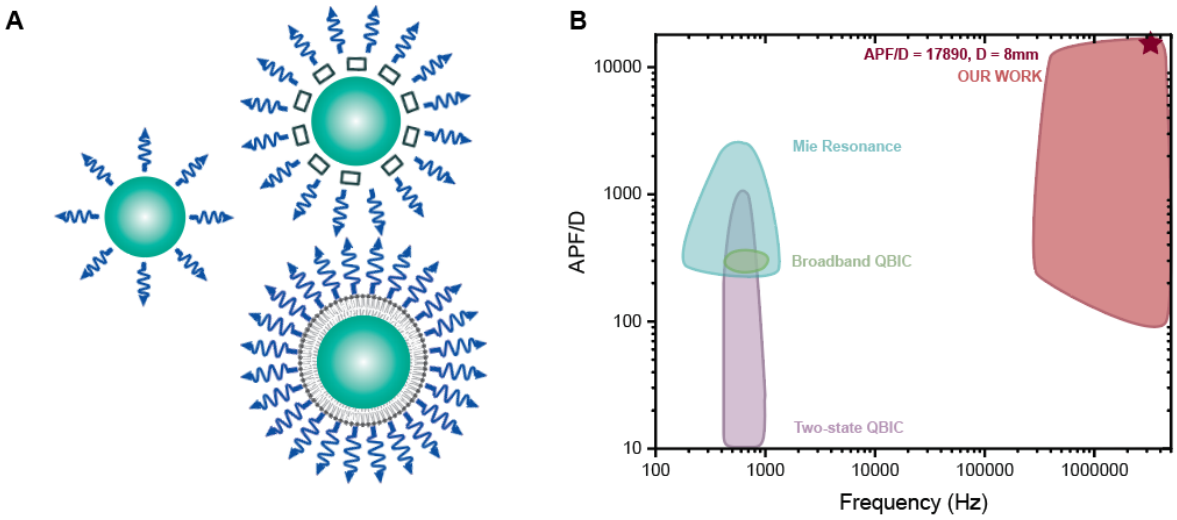

Fig. S5. (A) Schematic showing progression from a bare emitter (top left) to a cavity-enhanced resonator (top right), culminating in our perfluorocarbon nanodroplets (bottom), which act as reconfigurable nanoscale resonators. **(B)** Comparison of normalized acoustic Purcell factor per droplet diameter (APF/D) versus frequency. Our system diluted at a lower concentration (red star) achieves an APF/D of 17,890 at 8 mm, operating in an unprecedented high-frequency, high-efficiency regime.

Supplementary Materials 13

Effect of radiation impedance on Acoustic Purcell Factor (APF) and radiation efficiency of microbubbles.

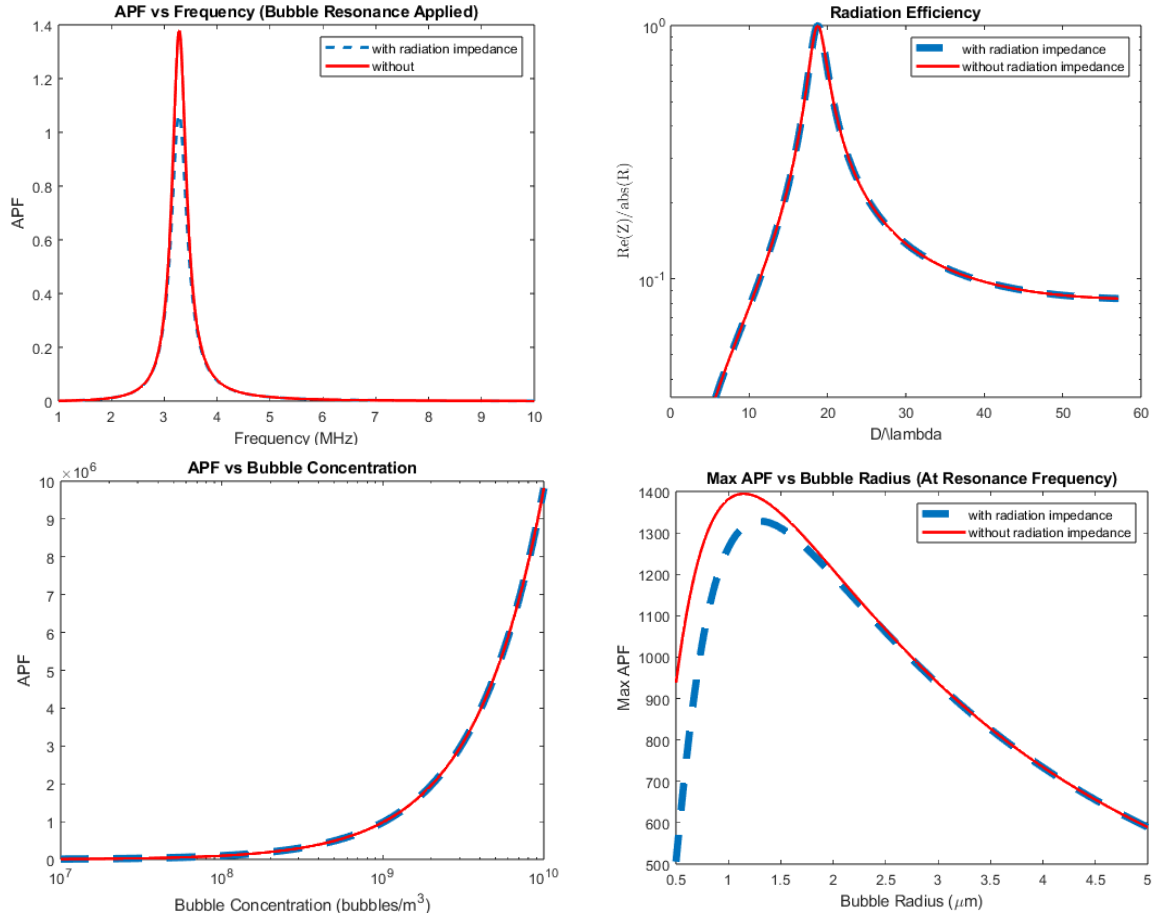

Fig. S6. (Top left) APF vs frequency under bubble resonance, comparing models with and without radiation impedance. Both show sharp resonance behavior with minimal deviation. **(Top right)** Radiation efficiency as a function of normalized bubble size (D/λ), demonstrating nearly identical behavior with and without radiation impedance, peaking near D/λ ≈ 15. **(Bottom left)** APF vs bubble concentration, showing exponential growth with increasing bubble number density, unaffected by radiation impedance. **(Bottom right)** Max APF vs bubble radius at resonance frequency, indicating a peak around ~1.5 μm. Radiation impedance slightly modifies the peak APF but does not significantly alter the overall trend.

Supplementary Materials 14

Microbubble accumulation and Acoustic Purcell Factor (APF) evolution during acoustic droplet vaporization (ADV).

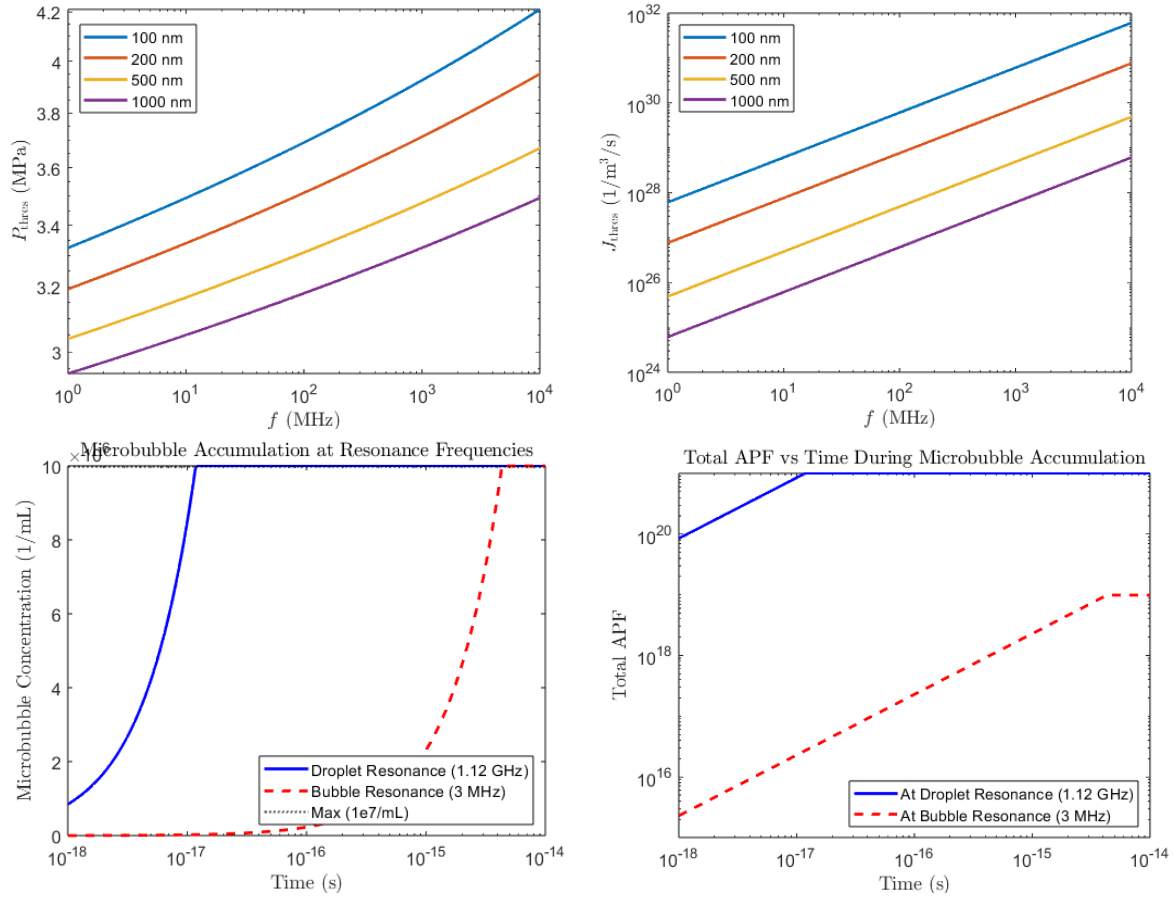

Fig. S7. (Top left) Threshold pressure vs frequency for nanodroplets of different radii (100–1000 nm). Smaller droplets require higher vaporization thresholds, with increasing dependence at higher frequencies. **(Top right)** ADV nucleation rate vs frequency for nanodroplets of varying radii, showing exponential growth with frequency and droplet size dependence. **(Bottom left)** Microbubble accumulation at resonance frequencies for droplet resonance (1.12 GHz, blue curve) and bubble resonance (3 MHz, red dashed curve). Microbubble concentration grows rapidly once vaporization is initiated, with a maximum limited at 10^7/mL. **(Bottom right)** Total APF vs time during microbubble accumulation at droplet resonance and bubble resonance. Droplet resonance drives earlier and stronger APF amplification compared to bubble resonance highlighting the enhanced reradiation efficiency enabled by the ADV process.

Supplementary Materials 15

Frequency response of the Acoustic Purcell Factor (APF) at different bubble concentrations

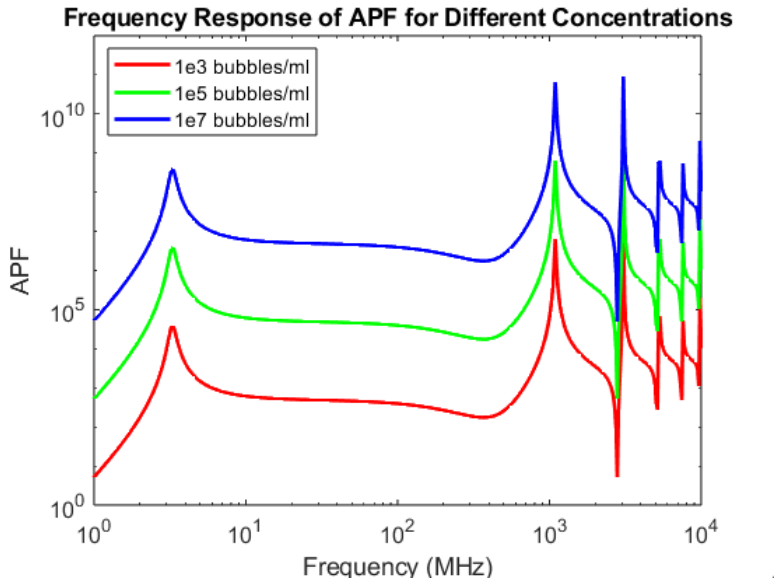

Fig. S7. APF spectra are shown for concentrations of 10^3 bubbles/mL (red), 10^5 bubbles/mL (green), and 10^7 bubbles/mL (blue). Increasing bubble concentration amplifies the APF across all frequencies, with multiple resonance peaks becoming more pronounced at higher concentrations. The results highlight how concentration strongly modulates both the magnitude and spectral distribution of APF, providing a tunable parameter for enhancing ultrasound emission and imaging performance.

Supplementary Materials 16

Total Acoustic Purcell Factor (APF) scaling with concentration at bubble and droplet resonance.

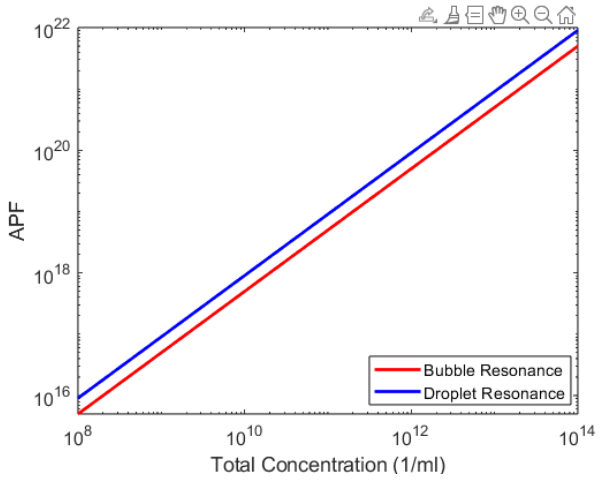

Fig. S8. APF increases linearly on a log–log scale with total concentration of scatterers from 10^8 to 10^{14} 1/mL. Both bubble resonance (red curve) and droplet resonance (blue curve) exhibit strong concentration dependence, with droplet resonance yielding slightly higher APF across the full range. This result highlights the dominant role of particle concentration in governing collective emission enhancement, complementing resonance-based tuning.

Supplementary Materials 17

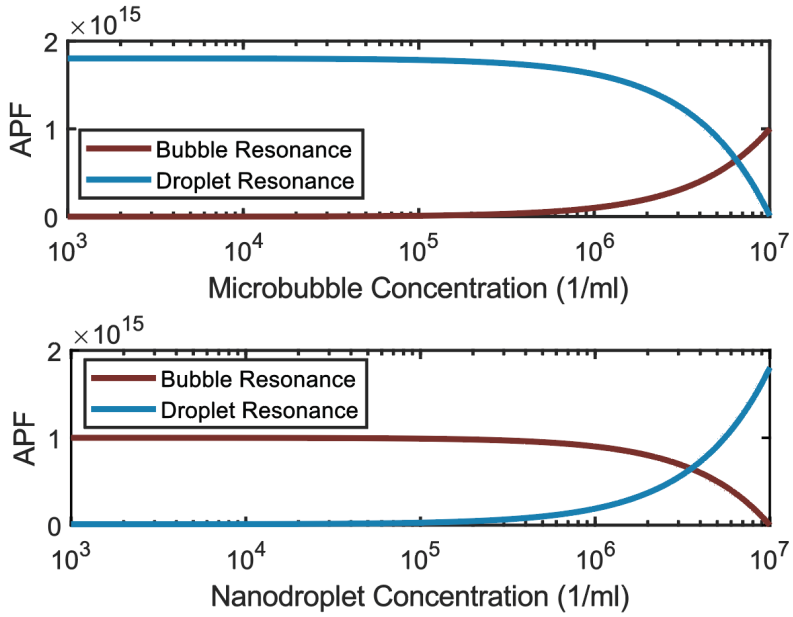

Fig. S9. APF evaluated at the droplet resonance (blue) and bubble resonance (brown) as the agent populations shift. Top: As microbubble concentration increases (i.e., progressive ADV of nanodroplets to bubbles), APF at the droplet resonance falls while APF at the bubble resonance rises, yielding a crossover where emission becomes bubble dominated. Bottom: As nanodroplet concentration increases (i.e., recondensation of bubbles back to droplets), the trend reverses and the spectrum becomes droplet-dominated. Concentrations are on a log scale (1 ml^{-1}). These curves illustrate how population balance enables tunable, agent-centric emission by steering APF between droplet- and bubble-resonant channels.

Supplementary Materials 18

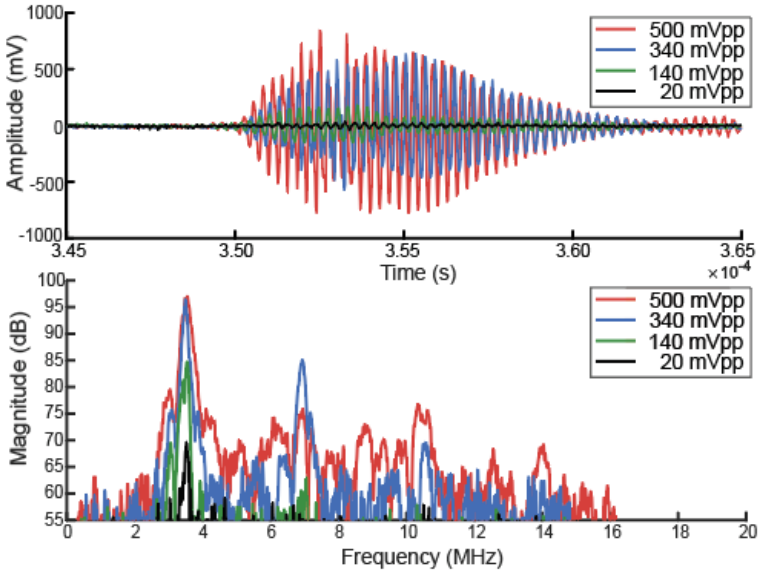

Fig. S10. Time and frequency domain of recorded RF signals at pre-PT (20mVpp), ADVI (140mVpp), ADVII (340mVpp), and IC (500mVpp) with PFCnDs inside gel sample.

Supplementary Materials 19

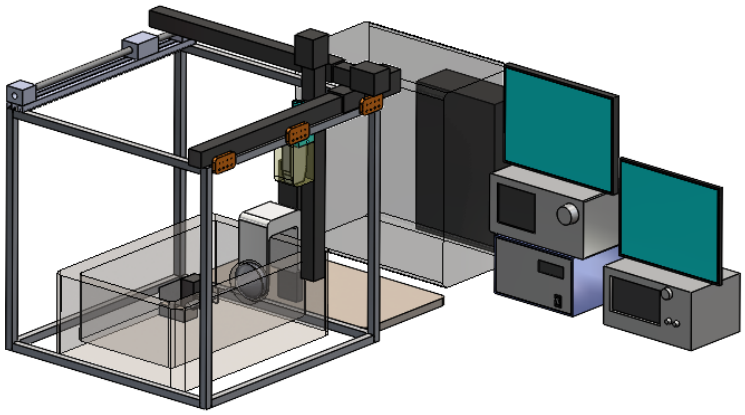

Fig. S12. Custom enclosure (aluminum-extrusion frame with clear panels) houses a temperature-controlled water tank and gel-phantom holder. A motorized X–Y–Z gantry positions the hydrophone or imaging transducer and moves relative to the sample and the focused-ultrasound (FUS) transducer. Instrument stack at right—PC/monitor, function generator, RF power amplifier, oscilloscope, and Verasonics system—provides drive, synchronization, and data acquisition.

Supplementary Materials 20

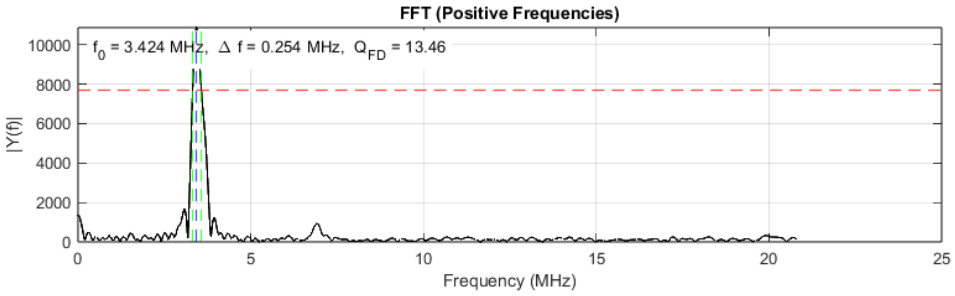

Fig. S13. FFT of the nanodroplet sample under a 3.5 MHz drive (280mVpp). The resonance peak is fit with a Lorentzian (green), giving a center frequency f0 = 3.424 MHz and a 3-dB bandwidth Δf3dB=0.254 MHz. The frequency-domain quality factor is then calculated to be 13.46.

Experimentally, the Quality factor (Q) for nanodroplet medium was found to be 13.49. Since we know that under resonance conditions,

$$A_2 = \frac{4\omega_0^2}{c_0^2} - \frac{12\rho_0 n\varepsilon}{9+4/Q^2},\ B_2 = \frac{8\rho_0 n\varepsilon}{9+4/Q^2}.$$

The attenuation coefficient and wave number follow:

$$\alpha_2 = \frac{1}{\sqrt{2}}\sqrt{\sqrt{A_2^2 + B_2^2} - A_2},$$

$$k_2 = \frac{B_2}{2\alpha_2}$$

Thus, for the nanodroplet sample at 280mvpp input at 3.5 MHz, we can calculate an attenuation coefficient to be:

$$\alpha_{2,\mathrm{ND}} = 5.446 \times 10^2 \sim \mathrm{m}^{-1} = 47.30 \sim \mathrm{dB/cm} \quad \sim 3.5 \sim \mathrm{MHz},$$

For pure water, the attenuation is:

$$\alpha_{\mathrm{H_2O}} = 0.007 \sim \mathrm{dB/cm} = 0.0806 \sim \mathrm{Np/m}$$

Therefore,

$$\frac{\alpha_{2,\mathrm{ND}}}{\alpha_{\mathrm{H_2O}}} = \frac{47.30}{0.007} = 6.76 \times 10^3$$

i.e., the nanodroplet sample has an attenuation coefficient 6.76×10^3 times larger than pure water at the same frequency (amplitude convention).